J Nanostruct 12(4): 1067-1074, Autumn 2022

RESEARCH PAPER

Nano-Hydroxyapatite Remineralization of In-Situ Induced Enamel Caries

Amer A Sultan [1], Mohanad Yakdhan Saleh [2], Emad Farhan Ali Alkhalidi [1]*

[1] Department of conservative dentistry, College of Dentistry, University of Mosul, Mosul, Iraq
[2] Department of chemistry, College of Education for pure Science, University of Mosul, Mosul, Iraq

ARTICLE INFO

Article History:
Received 27 May 2022
Accepted 15 September 2022
Published 01 October 2022

Keywords:
Biomineralization
Demineralization
Enamel
Nano-hydroxyapatite

ABSTRACT

Biological mineralization is the process by which living organisms form minerals to strengthen or harden existing tissues. It is considered a dynamic and complex lifelong process that is understood to be exceptionally common and is observed in all taxonomic kingdoms. Various structural features in mammals such as bone or enamel are the product of biomineralization. Controlling the process of biomineralization is considered the key to the future of conservative dentistry and the principle of minimally invasive dentistry. The purpose of the current research was to determine the effect of nano-hydroxyapatite (nano- HA) on the remineralization of *in-situ* induced enamel caries. The biomineralizing materials represented by nano-hydroxyapatite were synthesized from raw natural origin materials (bovine bones), the characteristics of this material were examined by, FTIR, XRD, SEM and FESEM before and after the remineralization of human teeth as a comparative study between the two materials. The XRD results displayed multiple diffraction peaks that indicate polycrystalline structures of the nanoparticles that compose the powder. The FTIR study resulted in bands at 562, 598, 960 and 1018 cm^{-1} belonging to phosphate groups $(PO4)_3$ were found. These functional groups are characteristic of hydroxyapatite. All images released from the SEM revealed clusters of nano-particles with hexagonal structures and different sizes ranging from 18 to 34 nanometers in dimension. The results reflected the significant role of the synthesized nano- HA in fortifying the enamel layer of human teeth. It concluded that the natural origin of synthetic nano- HA had the potential to produce an enamel-like layer.

How to cite this article
Sultan A A., Saleh M Y., Alkhalidi M F. Nano-Hydroxyapatite Remineralization of In-Situ Induced Enamel Caries. J Nanostruct, 2022; 12(4):1067-1074. DOI: 10.22052/JNS.2022.04.027

INTRODUCTION

Dental enamel is considered by far the human body's most rigid tissue, which exists as a means of shielding teeth from mastication and is one of the most important lines of defense against tooth decay. Unfortunately, mature enamel lacks the ability to self-regeneration or heal itself by a cellular repair mechanism when it is subjected to significant mineral loss during dental caries and chemical erosion [1]. However, it is now well recognized that the construction of incipient enamel caries is a reversible process where stages of development alternate with periods of remineralization [2]. The dominating components of the microstructure of human enamel are nano-sized hydroxyapatite particles and micron-

* Corresponding Author Email: mohanadalallaf@uomosul.edu.iq

structured enamel rods that bundle, by interlacing enamel interrod [3]. The enamel apatite is micro or nanocrystalline of varying composition with several distinct chemical characteristics that include non-stoichiometry, the Ca/P ratio ranges from 1.54 to 1.73, in comparison with 1.67 for synthetic apatite; impurities as structural substituents and surface pollutants, e.g., sodium, magnesium, iron, and other ions [4]. Regardless of the abundance of available materials in the dental markets poised to replace the enamel material, the aim to restore the biological structure of enamel remains a great challenge, enamel is not a living tissue [5]. Conventional commercial materials that are used to substitute enamel include amalgams, composite resins and ceramics and have proved to be substantially different from enamel in terms of chemical composition and crystal construction. Hence the features and appearance of these materials fail to match those of natural enamel. In addition to this, recurrent caries often develops in conjunction with these replacement materials due to unsatisfactory fitting, and weak adhesion to tooth structure. Furthermore, the weakly bonded interface may lead to the shedding of restorative materials, which could spell the failure of restoration and the requirement of further surgery [6-8].

Hydroxyapatite (HA) material is one of the most bioactive and biocompatible resources and is extensively used to coat artificial joints and tooth roots. Nano-HA particles have similarities in morphology, crystal structure and crystallinity to the apatite crystal of tooth enamel [9]. In the last few years, an increasing quantity of studies has revealed that nano-HA has the good potential to remineralize artificial carious lesions and incipient caries lesions [2]. *In situ* regeneration of hydroxyapatite on demineralized enamel surface could be considered the ideal result of enamel repair, due to the production of an enamel-like crystalline structure layer. For the time being, numerous systems have been tested for the regeneration of enamel material, including electrolytic deposition, hydrothermal synthesis, and the use of surfactants and hydrogen peroxide with varying findings [10-12]. However, these methods are considered extreme and usually undertaken in severe, which cannot be applied during routine clinical procedures [6, 13, 14].

Biomineralization is a process that produces non-living tissues and minerals such as bones, shells and teeth that have specific biological functions and structures [15]. These biominerals are characterized by reproducible and species-specific crystallochemical properties, which include uniform particle sizes, well-defined structures and compositions, high levels of spatial organization, complex morphologies, controlled aggregation and texture and preferential crystallographic orientation, high-order assembly into hierarchical structures [11, 1]. To date, there has been no reported research regarding the nano-HA remineralization of *in-situ* induced enamel caries, or which manifest the best defense under systems that imitate real-life situations. Therefore, the aim of this study was to evaluate the effect of the size of the HA biomaterial particles used to induce remineralization in human enamels subjected to artificial caries induction

MATERIALS AND METHODS

Collection of teeth samples

Noncarious human first premolars (extracted for orthodontic purposes) were provided by different orthodontic clinics in Mosul and subsequently collected to be used in this study. The use of human molar tissue specimens followed a protocol that was approved by the ethical committee of the college of dentistry at the University of Mosul and agreed upon by the patients involved. The collected specimens had no previous restorations; they were devoid of any developmental anomalies and were taken from patients who had no history of systemic diseases. Samples were cleansed by ultrasonic treatment in deionized water for 20 min after with silicon carbide paper (nos. 600 and 1200) and stored in thymol solution (0.2 wt %) at 4°C before use [16].

Bovine bone preparation

For this study, the raw material of choice was bovine femur bones obtained from a local butcher. As a commencement, the bovine bones were boiled in water for 2 hours as a means of defatting and streamlined removal of macroscopic adhering impurities. Thereafter, the bones were washed and cleaned carefully with water to clear them of all of the attached meat, tendons, bone marrows, and other soft tissues. The bones were then immersed in acetone for two hours and subsequently washed out with water for several times. The process was followed-up by drying said bovine bones to evaporate any absorbed water.

After that, the dried bovine bones were crushed into small pieces using a mortar pestle and then milled into smaller particle sizes utilizing a rotary mill (Fritsch, Germany). Finally, the bovine bones were sifted in the range of 45- 125μm using a sieve shaker (Retsch, Germany) [17, 18].

Calcination

In the calcination process, a select amount of 10 g of bone particles was placed in an open alumina crucible and heated up to 1200°C in a furnace (Carbolite, UK) to eliminate organic constituents that remained in the bovine bones, leaving only HAP. [17, 18].

Grinding and sieving

The powder that resulted from calcination was crushed and sieved to nano-sized particles by the ball milling machine method.

Characterization of the resultant powder

Fourier Transform Infra-Red Spectroscopy (FTIR)

Bruker ALPHA II FTIR Spectrometer was utilized to analyze the powder samples. FTIR results were undertaken to identify functional groups and their respective vibration modes present in the nano-HA samples. The analysis was carried out in spectra between 400-4000 cm^{-2} wavelength, to determine the quality and purity of the extracted powder.

X-Ray Diffraction Spectroscopy (XRD)

The diffractograms were acquired using Bruker D8 Advance Diffractometer, with copper Kα radiation (CuKα 1, 54056 Å), operating at 30 kV and 20 mA. where the spectrum is taken at 2θ: 20°–80° with an incremental step size of 0.04° and an acquisition speed of 1° min-1. The size of the crystals was determined according to the equation Scherrer [19]:

$$D = \frac{k\lambda}{\beta cos\theta} \quad (1)$$

where D is the crystallite size, k=0.9 is a correction factor to account for particle shapes, β is the full width at half maximum (FWHM) of (002) peak, λ is the wavelength of the radiation, and θ is the Bragg angle.

Preparation of Artificial Caries Lesion.

Teeth samples were decoronated just below the cementoenamel junction using a rotary machine with a diamond disc. The cervical surface of the teeth was covered with an acid-resistant light cure dam. To simulate early caries lesions, tooth enamel was etched with H_3PO_4 (37 wt %) for 30s.

Preparation of the remineralizing material

For the preparation of remineralizing material, 200 mg of nano HA and organic base compound were poured into 80 ml of ethanol and then ultrasonicated for 5 min. The gel-like material was gathered through centrifugation and washed with ethanol.

Enamel Remineralization

The remineralizing material was dropped onto the enamel surface, the samples were air-dried at 25°C for 5 min, resulting in the formation of a gel-like coated layer on the enamel. Afterwards, the enamel samples were immersed in a modified simulated oral fluid at pH 7.00 ± 0.03 at 37°C and were kept in an incubator for 48 hours. The repaired enamel windows were placed in a water ultrasound bath for 20 min, rinsed with water, and air-dried at 25°C before the examination.

FESEM Analysis

Morphological analysis of the enamel surface changes after the introduction of artificial caries and the application of the remineralizing materials, which was observed in a MIRA3 TESCAN Scanning Electron Microscope, at SEM MAG: 330 Kx, WD: 4.29 mm and View Field: 0.629mm. The electron acceleration voltage was 20 kV. The energy dispersive spectroscopy (EDS) attachment of the electron microscope was also used to determine the atomic composition of various powder samples.

RESULTS AND DISCUSSION

The XRD diffractogram for the prepared non-stoichiometric nano-HA powder samples is presented in Fig. 1. The diffractogram displays multiple diffraction peaks that indicate polycrystalline structures of the nanoparticles that compose the powder. The recognized peak positions in the patterns were recorded and matched with peaks reported in the database of the Joint Committee on Powder Diffraction Standards (JCPDS No. 09–0432). These highs were distinct representatives of pure hexagonal crystalline hydroxyapatite.

The highest peaks belonging to the prepared hydroxyapatite as shown at angles between

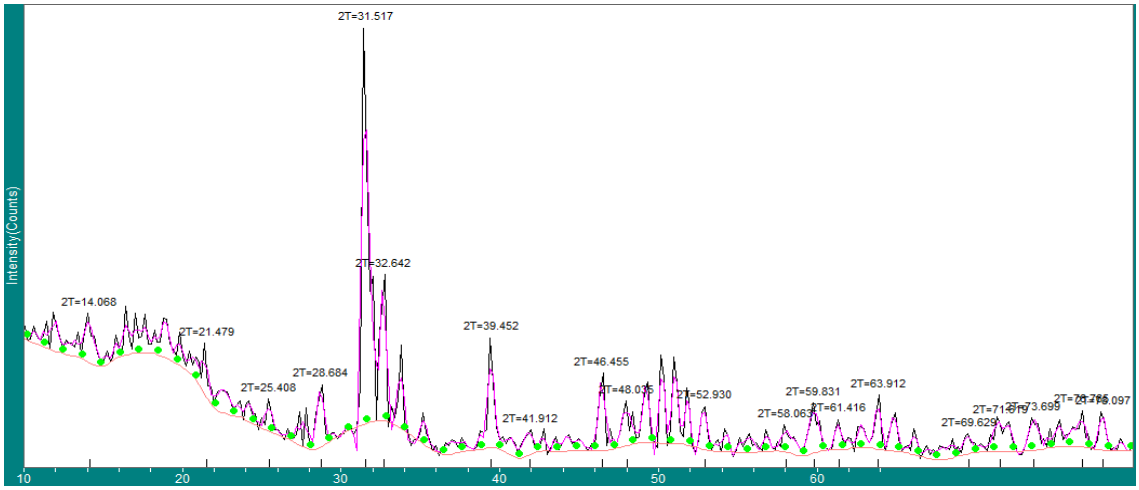

Fig. 1. XRD diffractogram for the prepared non-stoichiometric nano-HA powder

30°<2Θ°<33°, where a high peak is observed; and they are considered a characteristic of the x-ray diffraction pattern, and a "fingerprint" for the hydroxyapatite molecule. Nevertheless, these peaks are composed of two lines corresponding to crystalline hydroxyapatite at 31.517° and 32.642°. In addition, it was found that hydroxyapatite was present in a single base; it means that no other phases corresponding to another calcium phosphate as "α-phase calcium phosphate (α-TCP), β- phase of tricalcium phosphate (β-TCP), tetra calcium phosphate (TTCP)", among others, were found in the materials obtained. Therefore, it can be concluded that no HA mixing with

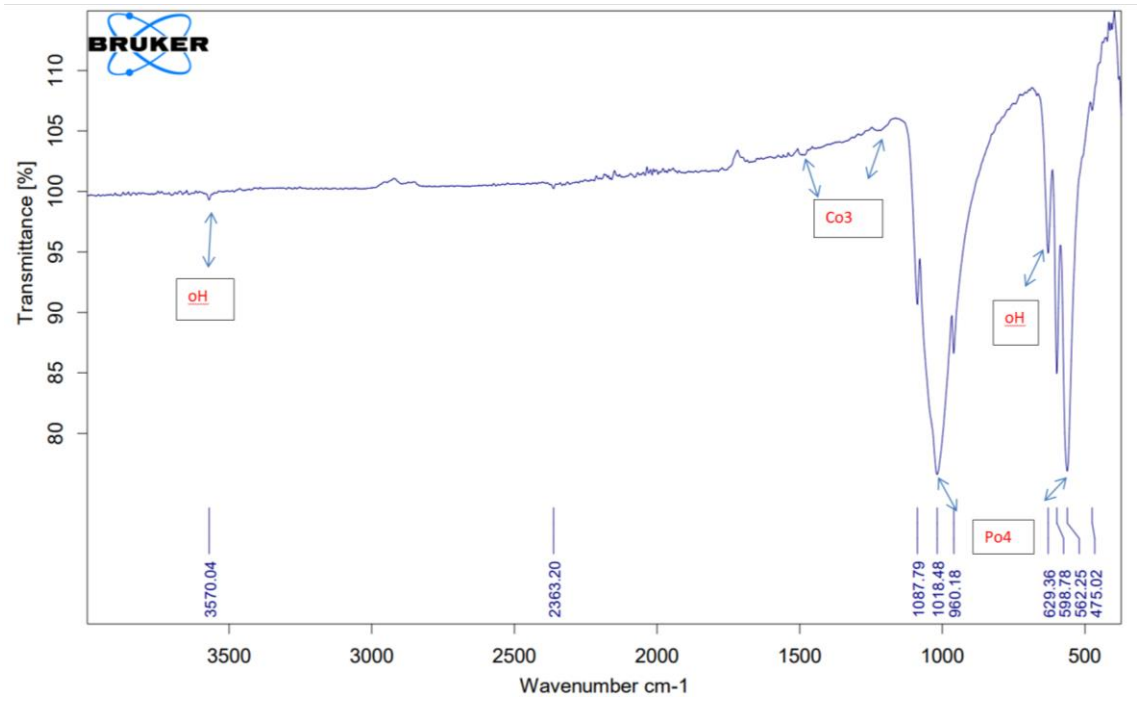

Fig. 2. The infrared spectra of the prepared HA

Table 1. typical vibrational bands of HAP

Functional Group	Vibrational mode	Wavenumber (cm^{-1})
OH^-	Stretch	3570
	Bending	629
PO_4^{3-}	Asymmetric bend	561 598
	Asymmetric stretch	1021 1087
	Symmetric stretch	961
CO_3^{2-}	Asymmetric stretch	1545 1450
	Symmetric bend	878

other crystalline compounds was discerned [20]; moreover, in these diffractograms, a preferential growth in the (211) plane at 2θ = 31.517° is observed. This is a typical characteristic of the HA.

The FTIR analysis was used to study the composition of the prepared HA powder in correspondence with that of standardized HA. Fig. 2 shows the infrared spectra of the prepared HA. In these spectra, bands placed at 629 and 3570 cm^{-1} corresponding to the hydroxyl (OH-) vibrational groups, can be identified [20,21]. Furthermore, bands at 562, 598, 960 and 1018 cm^{-1} belonging to phosphate groups $(PO_4)_3$ were found. These functional groups are characteristic of hydroxyapatite [22]. Table 1 presents a list of the functional groups, wavelength number and type of vibration mode [23].

Fig. 2 shows the transmittance intensity of the bands at 629 and 3570 cm-1 belonging to OH is lower in the case of the natural HA as compared to synthetic HA. This difference can be attributed to the fact that synthetic HA was obtained by means of reactions between two solutions in an aqueous environment, promoting the formation of a great quantity of this type of function; on the contrary, natural HA was obtained using physical reactions. With this method, the organic material of bones was extracted, to leave only the inorganic part corresponding to different calcium phosphate, mainly the HA. During this process, the material did not remain in contact with any aqueous solution, being the possible cause of no formation of the great number of hydroxyl groups [24].

In Fig. 2, bands at 1450 and 1545 cm^{-1} corresponding to carbonate groups are identified; moreover, in Table 1, the vibrational modes observed in the synthetic HA are listed. These bands are formed, this methodology, a carbonate HA was obtained. This type of HA exhibits a substitution of carbonate ions by hydroxyl ions (A type substitution) and carbonate ions by phosphate ions (B type substitution) [25]. This type of substitution favors the HA powder's bioactivity because the negative charge carriers initiate and promote the bone type apatite growth in presence of the SBF [26].

The prepared hydroxyapatite SEM images obtained under different magnifications revealed clusters of nano-particles with hexagonal structures and different sizes ranging from 18-34 nm in diameter. These particles are arranged in an aggregation that forms larger molecules due to high surface activities Fig. 3.

In regards, the enamel surfaces that were subjected to artificial caries induction showed a remarkable lost enamel prism core but retained periphery which result in the presence of small depressions due to dissolution of the prism ends. A few focal holes were also discerned. They alternated with smoother surfaces, where the depressions were poorly marked or even absent under a scale bar 20μm as shown in Fig. 4A. At higher magnifications (scale bar 1μm), the depressions appeared wedge-shaped. Detailed

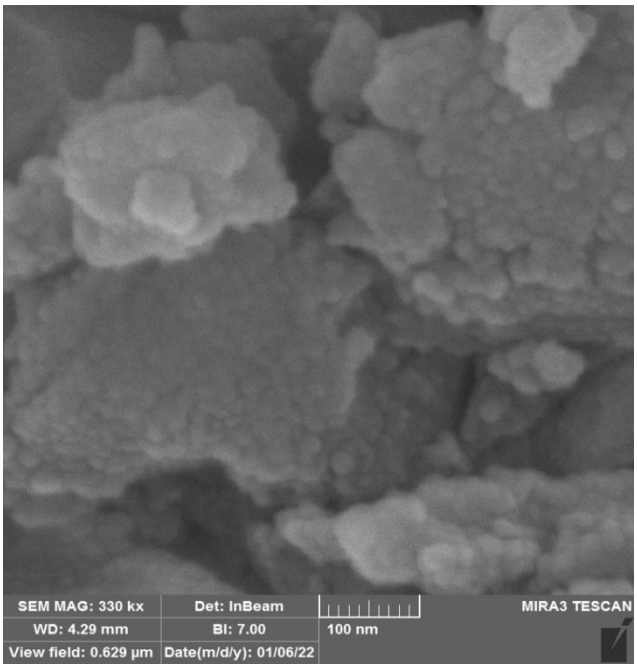

Fig. 3. SEM image of the prepared hydroxyapatite (Scale bar 100nm).

examination disclosed globular crystals which appeared less packed, resulting in varying degrees of intercrystalline spaces Fig. 4B.

The repaired enamel had the same morphological texture as native enamel because they were indistinguishable by SEM. The boundary between the repaired and native enamel demonstrates successful epitaxial growth and

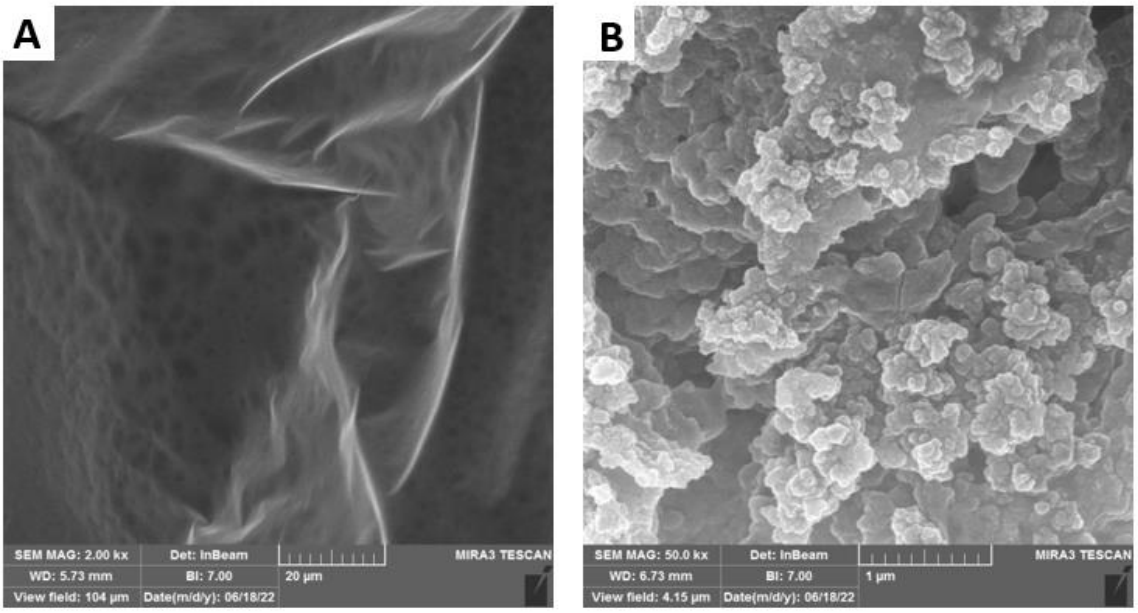

Fig. 4. (A) Demineralized enamel surface. (B) Demineralized enamel at higher magnification.

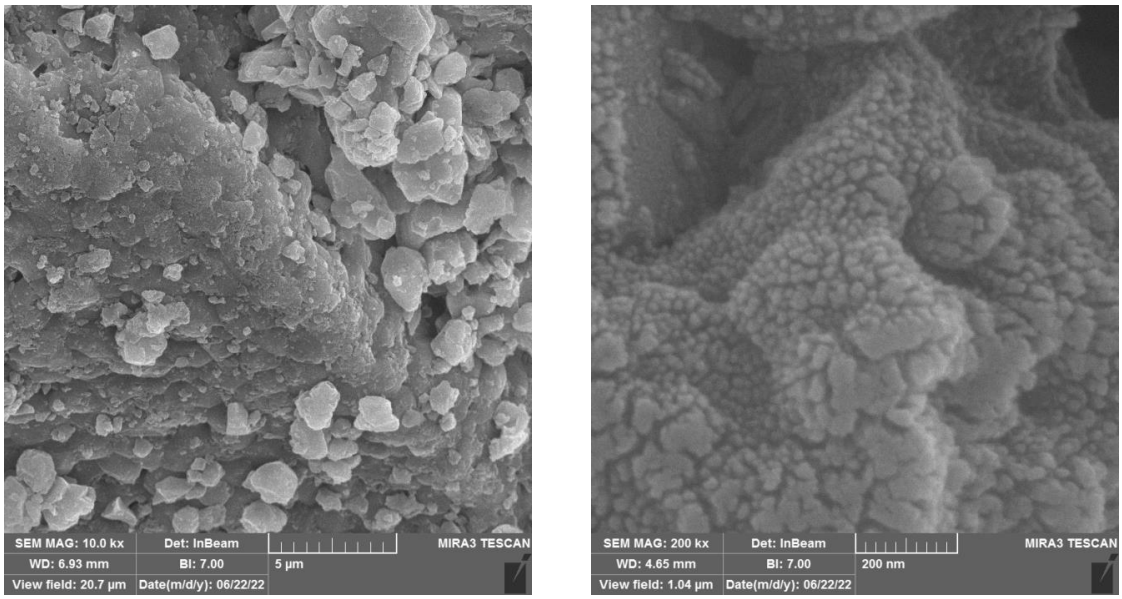

Fig. 5. Nano-HA repaired enamel at different magnifications (200nm right and 5µm left).

confirms the formation of a new HA layer. Notably, the resulting HA and the assembled structures in the repaired layer were precisely the same as the native materials. Although both enamel rods and inter rods are HA, they have different orientations in the enamel as shown in Fig. 5.

The EDS results confirm the non-stoichiometric nature of the prepared HD, with a Ca/p ratio of 1.622. The calcium deficiency prepared HA, was attributed to ionic substitutions of different types and amounts of elements like magnesium, strontium, sodium, and silicon. The natural HA found in bones and teeth is non-stoichiometric and displays variable deficiencies in Ca, P and OH. These deficiencies are made up of bionic substitutions of different types and amounts of elements like magnesium, strontium, sodium, and silicon [27]. The presence of these substitutions changes the structure and surface chemistry of HA, which in turn influences the biochemistry of bones, enamel, and dentin. The influence of these ionic species on hard tissues has not been fully elucidated. However, other studies revealed the presence and significance of small concentrations of silicon in osteoid regions of young mice and rats, which indicates the role of silicon in the early stages of bone formation and calcification [28]. Similar in vitro and in vivo studies have also shown the important role of silicon in the growth and development of hard tissues. Comparable studies have revealed the inclusion of magnesium in HA acts as a growth factor and stimulate osteoblast proliferation [29].

Both the enamel rods and inter-rods could be epitaxially grown simultaneously in the repair process as shown in Fig. 5. This coinstantaneous duplication of the HA with differential orientations during the enamel reconstruction means that each individual epitaxial growth process is specific and controllable at the nanoscale, affording a high structural resolution to benefit the construction of materials with complicated architectures. A cross-sectional SEM image reveals that the thickness of the enamel-identical repair layer was approximately 2.0 to 2.8 µm as appeared in Fig. 5, with well-organized and uniform characteristics. All diffraction peaks in the prepared HA and their relative intensities were identical to those of the original enamel HA, implying an identically organized crystallographic structure at the macroscopic level.

CONCLUSION

Nano-hydroxyapatite had the potential to remineralize initial enamel caries lesions. The precise remineralization of the enamel structure from the nanoscale to the macroscale was achieved. The repair of demineralized tooth enamel could be achieved by this biomimetic tactic since the nano-hydroxyapatite of proper resources

could be useful in promoting remineralization.

CONFLICT OF INTEREST

The authors declare that there is no conflict of interests regarding the publication of this manuscript.

REFERENCES

1. Tang S, Dong Z, Ke X, Luo J, Li J. Advances in biomineralization-inspired materials for hard tissue repair. International Journal of Oral Science. 2021;13(1).
2. Pepla E. Nano-hydroxyapatite and its applications in preventive, restorative and regenerative dentistry: a review of literature. Ann Stomatol (Roma). 2014.
3. Bismayer U, Shi J, Klocke A, Gierlotka S, Palosz BF. From Dental Enamel to Synthetic Hydroxyapaptite-Metal Composites. Key Eng Mater. 2005;288-289:561-564.
4. Pajor K, Pajchel L, Kolmas J. Hydroxyapatite and Fluorapatite in Conservative Dentistry and Oral Implantology—A Review. Materials. 2019;12(17):2683.
5. Ruan Q, Moradian-Oldak J. Amelogenin and enamel biomimetics. Journal of Materials Chemistry B. 2015;3(16):3112-3129.
6. Cao C, Mei M, Li Q-l, Lo E, Chu C. Methods for Biomimetic Mineralisation of Human Enamel: A Systematic Review. Materials. 2015;8(6):2873-2886.
7. Zhou Y, Zhou Y, Gao L, Wu C, Chang J. Synthesis of artificial dental enamel by an elastin-like polypeptide assisted biomimetic approach. Journal of Materials Chemistry B. 2018;6(5):844-853.
8. Pandya M, Diekwisch TGH. Enamel biomimetics—fiction or future of dentistry. International Journal of Oral Science. 2019;11(1).
9. Amaechi BT, Najibfard K, Chedjieu IP, Kasundra H, Okoye LO. Do Products Preventing Demineralization Around Orthodontic Brackets Affect Adhesive Bond Strength? The Open Dentistry Journal. 2018;12(1):1029-1035.
10. Ye W, Wang X-X. Ribbon-like and rod-like hydroxyapatite crystals deposited on titanium surface with electrochemical method. Mater Lett. 2007;61(19-20):4062-4065.
11. Abou Neel E, Aljabo A, Strange A, Ibrahim S, Coathup M, Young A, et al. Demineralization–remineralization dynamics in teeth and bone. International Journal of Nanomedicine. 2016;Volume 11:4743-4763.
12. Wei Y, Liu S, Xiao Z, Zhao H, Luo J, Deng X, et al. Enamel Repair with Amorphous Ceramics. Adv Mater. 2020;32(7):1907067.
13. Aulestia FJ, Groeling J, Bomfim GHS, Costiniti V, Manikandan V, Chaloemtoem A, et al. Fluoride exposure alters Ca^{2+} signaling and mitochondrial function in enamel cells. Science Signaling. 2020;13(619).
14. Liao Y, Chen J, Brandt BW, Zhu Y, Li J, van Loveren C, et al. Identification and Functional Analysis of Genome Mutations in a Fluoride-Resistant Streptococcus mutans Strain. PLoS One. 2015;10(4):e0122630.
15. Amaechi BT, Alshareif DO, Azees PAA, Shehata MA, Lima PP, Abdollahi A, et al. Anti-caries evaluation of a nano-hydroxyapatite dental lotion for use after toothbrushing: An in situ study. J Dent. 2021;115:103863.
16. Peng J, Lei L, Xiao H, Yang D, Zheng J, Zhou Z. Restoration of enamel anti-wear properties via remineralization: Role of occlusal loading. Friction. 2022;10(11):1838-1850.
17. Mohd Pu'ad NAS, Koshy P, Abdullah HZ, Idris MI, Lee TC. Syntheses of hydroxyapatite from natural sources. Heliyon. 2019;5(5):e01588.
18. Arokiasamy P, Al Bakri Abdullah MM, Abd Rahim SZ, Luhar S, Sandu AV, Jamil NH, et al. Synthesis methods of hydroxyapatite from natural sources: A review. Ceram Int. 2022;48(11):14959-14979.
19. Figueiredo M, Henriques J, Martins G, Guerra F, Judas F, Figueiredo H. Physicochemical characterization of biomaterials commonly used in dentistry as bone substitutes-Comparison with human bone. Journal of Biomedical Materials Research Part B: Applied Biomaterials. 2009;92B(2):409-419.
20. Al-Abboodi A, Mhouse Alsaady HA, Banoon SR, Al-Saady M. Conjugation strategies on functionalized iron oxide nanoparticles as a malaria vaccine delivery system. Bionatura. 2021;3(3):2009-2016.
21. Jabber Al-Saady MAA, Aldujaili NH, Rabeea Banoon S, Al-Abboodi A. Antimicrobial properties of nanoparticles in biofilms. Bionatura. 2022;7(4):1-9.
22. Raya I, Mayasari E, Yahya A, Syahrul M, Latunra AI. Shynthesis and Characterizations of Calcium Hydroxyapatite Derived from Crabs Shells (Portunus pelagicus) and Its Potency in Safeguard against to Dental Demineralizations. International Journal of Biomaterials. 2015;2015:1-8.
23. Bienenstock A, Posner AS. Calculation of the X-Ray intensities from arrays of small crystallites of hydroxyapatite. Archives of Biochemistry and Biophysics. 1968;124:604-607.
24. Aldujaili NH, Banoon SR. ANTIBACTERIAL CHARACTERIZATION OF TITANIUM NANOPARTICLES NANOSYNTHESIZED BY STREPTOCOCCUS THERMOPHILUS. Periódico Tchê Química. 2020;17(34):311-320.
25. Sossa PAF, Giraldo BS, Garcia BCG, Parra ER, Arango PJA. Comparative study between natural and synthetic Hydroxyapatite: structural, morphological and bioactivity properties. Matéria (Rio de Janeiro). 2018;23(4).
26. Liu Y, Shen Z. Dehydroxylation of hydroxyapatite in dense bulk ceramics sintered by spark plasma sintering. J Eur Ceram Soc. 2012;32(11):2691-2696.
27. Eliaz N, Metoki N. Calcium Phosphate Bioceramics: A Review of Their History, Structure, Properties, Coating Technologies and Biomedical Applications. Materials. 2017;10(4):334.
28. Price CT, Koval KJ, Langford JR. Silicon: A Review of Its Potential Role in the Prevention and Treatment of Postmenopausal Osteoporosis. Int J Endocrinol. 2013;2013:1-6.
29. Rattan S, Fawcett D, Poinern GEJ. Williamson-Hall based X-ray peak profile evaluation and nano-structural characterization of rod-shaped hydroxyapatite powder for potential dental restorative procedures. AIMS Materials Science. 2021;8(3):359-372.